18TH WORLD CONFERENCE ON EARTHQUAKE ENGINEERING
WCEE2024
MILAN

MILAN, ITALY
30TH JUNE - 5TH JULY 2024

www.wcee2024.it

SHAKING TABLE TESTS OF A 3-STOREY SELF-CENTRING STEEL MRF: PRELIMINARY ANALYSIS AND DESIGN

E. Elettore[1], F. Freddi[2], M. Latour[1], L. Pieroni[2], S. Di Benedetto[1], F. Gutierrez Urzua[2], A. B. Francavilla[1], B. Simpson[3], A. R. Barbosa[4], S. Ramhormozian[5], D. Grant[6], G. Rizzano[1], F. L. Ribeiro[7], A. A. Correia[7]

[1] University of Salerno, Salerno, Italy, eelettore@unisa.it

[2] University College London, London, UK

[3] Stanford University, Stanford, USA

[4] Oregon State University, Corvallis, USA

[5] Auckland University of Technology, Auckland, New Zealand

[6] ARUP, London, UK

[7] National Laboratory for Civil Engineering (LNEC), Lisbon, Portugal

Abstract: *Traditional seismic design methods, suggested by current codes and conventionally applied worldwide, rely on damage to building structures to dissipate the seismic input energy. This strategy allows meeting the life safety requirements but often results in post-earthquake scenarios where building structures are severely damaged with significant direct and indirect losses strongly affecting the overall resilience of communities. To address this issue, nowadays' earthquake engineering is facing an extraordinarily challenging era to provide more widely affordable, high-seismic-performance structures capable of sustaining the design earthquake intensity with limited socio-economic losses. To this end, the ERIES-SC-RESTEEL (i.e., Self-Centring seismic-RESilient sTEEL structures) project investigates the structural response, repairability, resilience, and performance recovery of steel low-damage self-centring moment-resisting frames, including friction devices and post-tensioned bars with disk springs at column bases and beam-to-column joints. A wide range of shaking table tests will be carried out at LNEC (Laboratório Nacional de Engenharia Civil) in Lisbon, Portugal, investigating the performance of a large-scale 3D three-storey steel moment-resisting frame with low-damage self-centring joints considering different properties and placements of the self-centring connections. As part of the ERIES-SC-RESTEEL project, this paper presents the preliminary numerical work for the design of the experimental tests. Advanced numerical models of the test specimen have been developed in OpenSees to perform non-linear time history analyses considering various design configurations, ground motion records and seismic intensities. The results provide useful insights for the design of shaking table tests and the expected experimental outcomes.*

1. Introduction

Earthquakes are among the deadliest and costliest catastrophic events worldwide. Conventional seismic design methods, suggested by most current codes (*e.g.,* Eurocode 8) and conventionally applied worldwide, rely on the construction damage to dissipate the seismic input energy and meet the life safety requirements. However, this design approach typically results in post-earthquake scenarios where building structures are severely damaged with considerable direct (*e.g.,* casualties, repair cost) and indirect (*e.g.,* downtime) losses as a consequence of 'rare' seismic events. This situation strongly affects the overall resilience of communities subjected to extreme seismic events, especially when damaged structures include strategic facilities that must remain operational in the aftermath of a damaging earthquake.

To overcome these drawbacks, nowadays' earthquake engineering is facing an extraordinarily challenging era coping with the task of providing seismic-resilient structures chasing the objectives of minimising both seismic damage and repair time, hence allowing limited socio-economic losses after severe earthquakes. To this end, the use of seismic devices has emerged as an efficient strategy, and some of these have been widely investigated and are nowadays used in construction. Some consolidated solutions include the use of passive energy dissipation devices (*e.g.,* Symans *et al.* 2008; Seo *et al.* 2014; Gioiella *et al.* 2018; Gutiérrez-Urzúa and Freddi 2022) and base isolation systems (*e.g.,* Grant *et al.* 2004; Dall'Asta *et al.* 2022). However, other innovative solutions, such as the use of rocking and spine low-damage systems (*e.g.,* Ricles *et al.* 2001; Simpson *et al.* 2023), have emerged in the last few years, showing several advantages. For steel Moment Resisting Frames (MRFs), the use of Friction Devices (FDs) in Beam-to-Column Joints (BCJs) (*e.g.,* Grigorian *et al.* 1993; MacRae *et al.* 2010; Latour *et al.* 2018; Di Benedetto *et al.* 2022; Li *et al.* 2023) has been widely investigated as a promising strategy able to provide both high local ductility and energy dissipation capacity with only minor yielding and wearing within replaceable elements. However, it has been demonstrated that the reduction of structural damage does not automatically entail repairability because of possible post-earthquake residual drifts, exceeding the commonly accepted limits (*i.e.,* 0.5% for buildings' repairability according to McCormick *et al.* 2008 or 0.2% for structural realignment according to FEMA P58-1).

This issue has been tackled by several research works introducing elastic restoring forces able to regulate the structure's Self-Centring (SC) capability. The use of SC systems has been proven as an effective strategy to reduce residual deformations and has been investigated in many different structural configurations and materials, including bridge piers (*e.g.,* Shen *et al.* 2022; Piras *et al.* 2022), RC structures (*e.g.,* Kurama *et al.* 2006), timber structures (*e.g.,* Pei *et al.* 2019; Blomgren *et al.* 2019), steel braced (*e.g.,* O'Reilly and Goggins 2021; Lettieri *et al.* 2023) and moment-resisting frames (e.g., Ricles *et al.* 2001, Garlock *et al.* 2007; Freddi *et al.* 2017; Elettore *et al.* 2021a). For steel MRFs one possible solution is the inclusion of self-centring devices at BCJs (*e.g.,* Ricles *et al.* 2001; Kim *et al.* 2009). In these systems, beams are usually clamped to the columns through Post-Tensioned (PT) steel bars parallel to the beams and anchored outside the connection, allowing the control of gap-opening mechanisms (*i.e.,* rocking) at BCJs. The seismic energy dissipation is provided by replaceable dissipative devices, *e.g.,* yielding set angles or FDs (*e.g.,* Christopoulos *et al.* 2002) included in the self-centring connection.

Furthermore, it has been demonstrated that Column Bases (CBs) play a fundamental role in the self-centring capacity of MRFs, and their protection is paramount to achieving structural resilience (*e.g.,* Elettore *et al.* 2023). To overcome the drawbacks of conventional CBs, several novel configurations have been proposed in the last few decades, based on the use of dissipative partial-strength joints equipped with FDs (*e.g.,* MacRae *et al.* 2009; Zhang *et al.* 2023) or combining such devices and SC systems (*e.g.,* Freddi *et al.* 2017; Kamperidis *et al.* 2018; Latour *et al.* 2019). For example, Freddi *et al.* 2017 presented and experimentally investigated (Freddi *et al.* 2020) a rocking damage-free steel CB equipped with FDs and high-strength steel PT bars. Similarly, Latour *et al.* 2019 proposed and experimentally studied a novel Self-Centring CB (SC-CB) consisting of a rocking column splice joint with a combination of FDs and PT bars with disk springs. Component tests of an isolated SC-CB specimen subjected to cyclic loads demonstrated a 'good' and stable flag-shaped hysteretic behaviour with negligible residual deformations. This connection is characterised by several advantages, such as: *1)* easy to construct and economically comparable with conventional joints; *2)* self-centring capability obtained with elements (*i.e.,* PT bars and disk springs) which have a size comparable to the size of the joint (*i.e.,* no need for long PT bars); *3)* the moment-rotation hysteretic behaviour of the components can be easily calibrated.

However, although several studies on such SC structures have been made in the last few years, demonstrating the advantages of these technologies, there is a significant need for advanced studies to reflect academic research in policy-making and building codes, hence promoting the application of these solutions in practice. In this direction, based on the connection typology proposed by Latour *et al.* 2019, a comprehensive investigation has been carried out for the definition of design strategies (Elettore *et al.* 2021a), extensive numerical simulations to investigate the global response of the structure (Elettore *et al.* 2021b), advanced 3D numerical simulations to investigate the local response of the connection (Elettore *et al.* 2022), and large scale Pseudo-Dynamic (PsD) tests to experimentally investigate the seismic performance and repairability of the system (Elettore *et al.* 2023). The large-scale experimental campaign was performed at the University of Salerno and focused on a 2-storey steel structure equipped with low-damage BCJs (*i.e.,* friction-based and dissipative but not self-centring) and SC-CBs. Further insights were developed regarding the system's reparability. The results of these studies demonstrated the benefits of the SC-CBs in minimising the residual interstorey drifts and the repair method's effectiveness in terms of enhanced repairability and resilience.

Moreover, most past studies on this topic demonstrated the beneficial effects gained in damage and residual drift reduction by including SC devices at all BCJs and CBs (*e.g.* Freddi *et al.* 2017). However, this solution may represent a limit to the practical application due to increased structural complexity. To address this issue, Pieroni *et al.* 2022a,b numerically investigated the influence of the placement of Self-Centring BCJs (SC-BCJs) within an 8-storey case-study steel MRF. Results demonstrated that significant advantages can be obtained by considering the effective placement of a limited number of SC-BCJs, representing the optimum compromise between structural complexity and seismic performance.

Although several aspects concerning the design, performance and repairability of such structures have been investigated, several open issues still need to be addressed. Moreover, for such innovative systems, there is a wide availability of proof-of-concept studies; however, large-scale shaking table tests are very limited (*e.g.,* Wang *et al.* 2022, Pampanin *et al.* 2023).

Within this context, the ERIES-SC-RESTEEL (Self-Centring seismic-RESilient sTEEL structures) project aims to advance knowledge and innovation by experimentally investigating the seismic performance, repairability, and effective placement of SC devices within steel MRFs. This solution is based on dissipative and SC components to be included at CBs and BCJs to dissipate the earthquake input energy and prevent residual drifts. The proposed research will perform a wide range of shaking table tests of a large-scale three-storey steel MRF with SC-BCJs and SC-CBs, considering different placements of SC connections. The shaking table tests will be carried out at LNEC (Laboratório Nacional de Engenharia Civil) in Lisbon, Portugal, and aim to investigate the seismic performance of the structure but also evaluate the repairability (including the repair time) and the performance of the repaired structure through repeated tests. The research aims to further expand the results obtained in Elettore *et al.* 2023, overcoming some of the limitations of the PsD testing procedures previously used. In particular, the shaking table tests will allow: 1) assessing the influence of the impacts at the rocking interfaces, potentially inducing local damages in the connections and affecting the effective damping of the system (PsD tests only numerically simulate the damping); 2) assessing the influence of the vertical component of the ground motion on the self-centring capacity of the CBs; 3) defining quantitative measures for the repairability of the structures (*e.g.,* repair time) and seismic performance of the repaired structures considering a large number of scenarios (the long time required for PsD tests does not allow investigating a large set of cases). This paper illustrates the preliminary design of the test specimen, the test programme and the preliminary numerical analyses carried out on the structure. A numerical Finite Element (FE) model of the test specimen is developed in OpenSees (Mazzoni *et al.* 2009), and non-linear dynamic analyses are performed to investigate the performance of the structure considering three different distributions of low-damage and low-damage self-centring joints.

2. Test specimen

2.1. Design of the specimen

The prototype structure is illustrated in Figure 1(a). It is characterised by three storeys and three bays in the x- and y-directions. The seismic-resistant part comprises four MRFs in both directions (i.e., highlighted in red), while the internal part comprises gravity frames. The interstorey heights are equal to 3.20 m at the first storey and 3.00 m at the higher storeys, while the longitudinal and transversal bays have span lengths equal to 5.83 m and 6.66 m, respectively. The scaled structure is illustrated in Figure 1(b). The model scaling is based on

the material and acceleration scaling identity, and a scaling factor equal to λ = 0.6 was selected to respect the Lab constraints and, at the same time, correctly reproduce the seismic response of the joints. The interstorey heights are equal to 1.92 m at the first storey and 1.80 m at the intermediate storeys, while the longitudinal and transversal bays have span lengths equal to 3.50 m and 4 m, respectively. The assumed floor system is a HI BOND A55/P600 steel-concrete composite floor. The design is carried out following the Eurocode 8 provisions.

The design earthquake at Ultimate Limit State (ULS) is defined considering the Type 1 elastic response spectrum with a PGA equal to 0.35g and soil type D. The Collapse Limit State (CLS) is assumed to have an intensity equal to 150% of the ULS. The behaviour factor based on the Eurocode 8 for MRFs in DCH is assumed as q = 6.5. The interstorey drift limit for the Damage Limit State (DLS) is assumed to be 1% for non-structural elements fixed in a way such as not to interfere with structural deformations. The specimen to be tested is illustrated in Figure 1(c). The preliminary design indicates that the floor masses of the specimen to carry out the test are equal to 11.76 and 10.31 tons at intermediate floors and the roof, respectively. Hence, the total mass of the specimen is equal to 33.82 tons, which is compatible with the specific equipment available at the research infrastructure. Beams' and columns' cross-sections are IPE240 and HEB180, with steel grade S355. The two MRFs will be equipped with the previously presented low-damage BCJs and CBs, with and without PT bars. The presence of the PT bars provides the joints with the SC capability, and different SC joints' placement along the height of the structure will be evaluated. For the sake of clarity, hereinafter, low-damage (LD) joints without PT bars are referred to as LD-BCJs and LD-CBs, while joints with PT bars are referred to as SC-BCJs and SC-CBs.

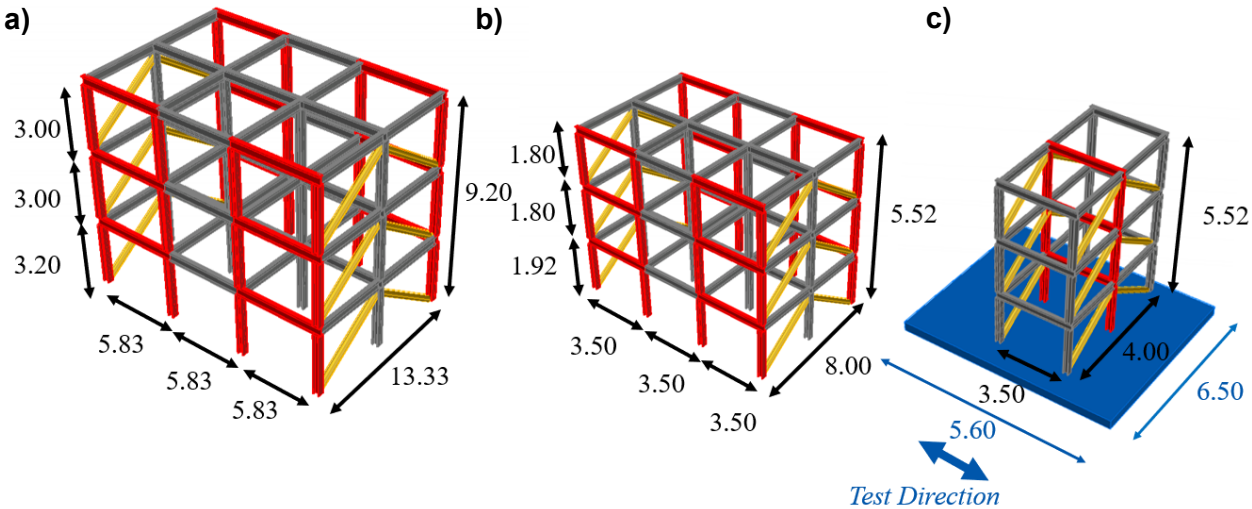

Figure 1. 3D view & geometries of: a) Prototype; b) Scaled Structure. c) Test Specimen. [Dimension in m].

2.2. Design of the Beam-to-Column Joint (BCJ)

Figure 2 illustrates the Beam-to-Column Joint (BCJ) with and without PT bars: *i.e.,* the SC-BCJ in Figure 2(a) and the LD-BCJ in Figure 2(b). In both configurations, the beam is connected by a combination of FDs, which dissipate the seismic input energy through the alternate slippage of the surfaces in contact. The FDs consist of properly coated steel friction shims and steel cover plates clamped with pre-loadable bolts. The FDs are characterised by a rigid-plastic hysteretic model, which depends on the clamping force and the friction coefficient μ of the contact interfaces.

In the SC-BCJ, the self-centring system is composed of PT bars symmetrically placed with respect to the column's depth and arranged in series with a system of disk springs. The disk springs are arranged in series and parallel, acting as a macro-spring system, ensuring an adaptable stiffness-resistance combination to the self-centring system. The disk springs in parallel control the yielding resistance of the SC system, while the disk springs in series control its stiffness. The dimensions of the slotted holes are designed to accommodate the target rotation (assumed equal to 0.04 rads).

In addition, Figure 2 shows the schematic representation of both connections, including the expected forces during the gap-opening around the centre of rotation (COR) and the moment-rotation behaviour. In the case

of SC-BCJs, the moment-rotation behaviour is the typical flag-shape curve, represented in Figure 2(a), where M_1 is the moment at the gap opening, and M_2 is the moment at the target rotation. Conversely, in the case of the LD-BCJ, the moment-rotation behaviour is a hysteretic rectangular curve where M_{Slip} is the slippage moment of the FDs, and M_t is the moment at the target rotation. The connections will be tested with and without PT bars. The presence of the PT bars provides the joints with self-centring capability, and different SC joints' placement along the height of the structure will be evaluated.

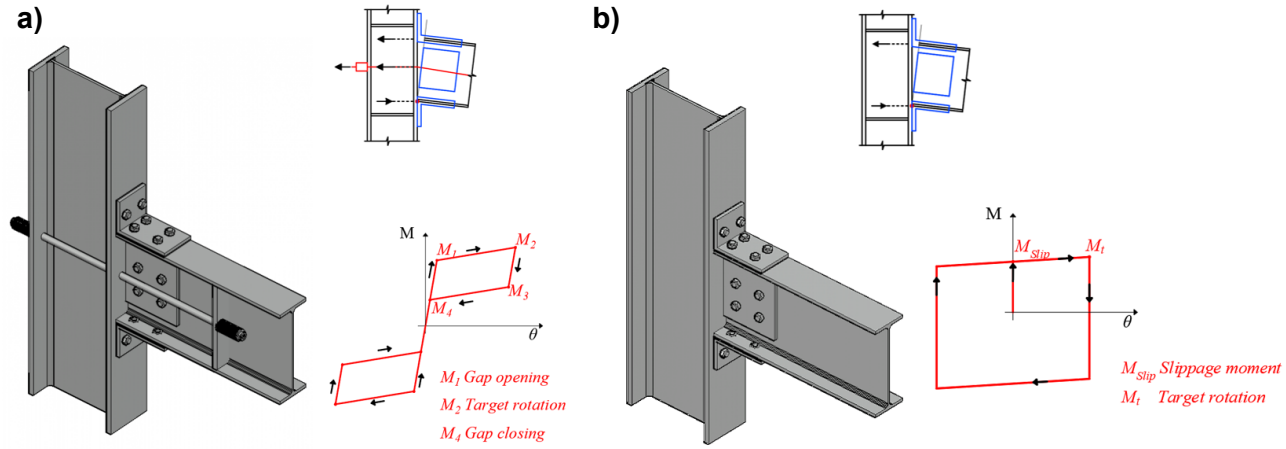

Figure 2. 3D view & moment rotation behaviour of: a) SC-BCJ; b) LD-BCJ.

2.3. Design of the Column Base (CB) connection

Figure 3 illustrates the Column Base (CB) connection with and without PT bars: *i.e.,* the SC-CB in Figure 3(a) and the LD-CB in Figure 3(b). Similarly to the BCJ, in both configurations, the column is connected by a combination of FDs and a SC system composed of PT bars arranged in series with disk springs. The same structural details (*i.e.,* oversized holes and flange slots) are designed to accommodate the target rotation (assumed equal to 0.04 rads). In addition, Figure 3 shows the schematic representation of both connections, including the expected forces during the gap-opening around the COR and the moment-rotation behaviour. In the case of the SC-BCJ, the moment-rotation behaviour is the typical flag-shape curve, represented in Figure 3(a), where M_1 is the moment at the gap opening. Conversely, in the case of LD-BCJs, the moment-rotation behaviour is a hysteretic rectangular curve where M_{Slip} is the slippage moment of the FDs.

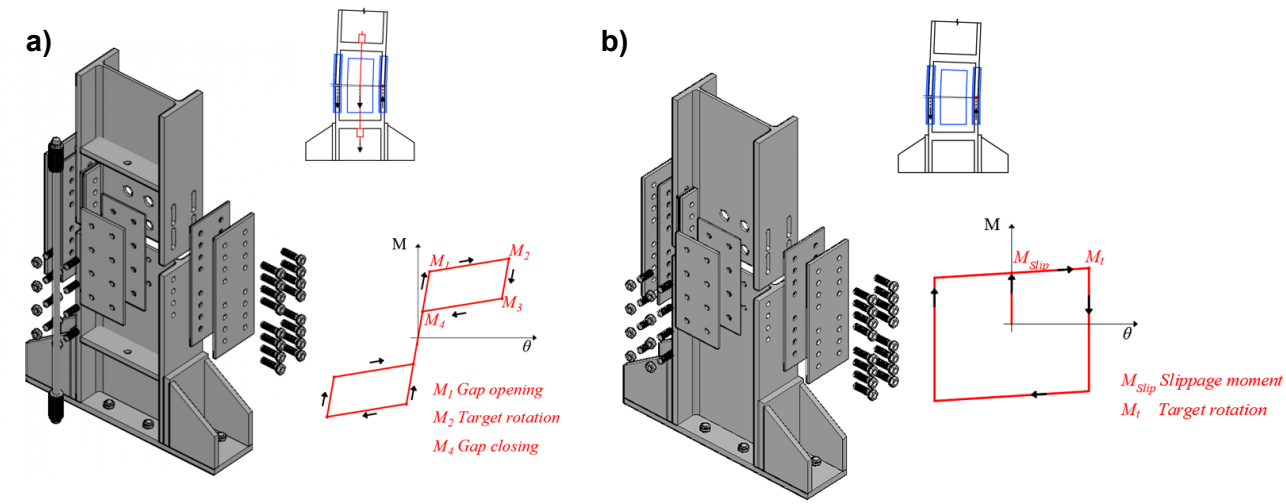

Figure 3. 3D view & moment rotation behaviour of: a) SC-CB; b) LD-CB.

3. Test programme

Table 1 summarises the proposed test programme. Preliminarily, the programme investigates the local behaviour of materials and components (Tests 1 & 2). This includes steel coupons, friction shims, PT-bars

with disk springs, and a limited number of sub-assemblies, such as LD-BCJs/SC-BCJs and LD-CBs/SC-CBs (without/with PT bars). Some preliminary tests will be conducted at the University of Salerno. Past findings on the characterisation of the friction materials and joints will be considered to minimise the need for additional tests/prevent duplication of previous work (Latour *et al.* 2018). In the second phase, the proposed mock-up, considering different layouts of the SC joints' placement along the height of the structure (Test 3), will undergo shaking table tests. For each configuration, a characterisation of the mock-up's dynamic response will be initially conducted through white noise tests to estimate damping ratios and natural periods. Subsequently, shaking table tests will be performed to evaluate the seismic performance, SC capacity, and repairability of the structure after each test. The tests will be performed using different accelerograms and incremental intensities ranging from the DLS to the CLS. For the selected configurations, additional tests will be performed with and without the vertical components of the ground motion records and, for some cases, repeated tests will be performed to evaluate the reliability of results (Test 4).

Table 1. Proposed test programme.

Test	Description
1	Material/components characterisation tests, coupon tests, double lap-shear friction joints, tests on PT bars with disk springs.
2	Subassemblies characterisation: 1 test on SC-BCJ and 1 test SC-CBs with/without PT bars with different levels of prestressing.
3	Shaking table tests of the mock-up with different placement of the self-centring devices
4	Additional tests with/without vertical ground motions and repeated tests for reliability assessment.

4. Numerical Modelling

2D non-linear FE models are developed in OpenSees (Mazzoni *et al.* 2009) (Figure 4). Three models are proposed: 1) the MRF equipped with LD-BCJs and LD-CBs (*i.e.,* LD-MRF); 2) the MRF with LD-BCJs and SC-CBs (*i.e.,* LD-MRF-CB); 3) the MRF with SC-CBs and SC-BCJs (*i.e.,* SC-MRF). Preliminary numerical simulations are carried out to investigate and compare the seismic performances of the structures equipped with different connection typologies and to check the compatibility with the capacities of the test equipment.

4.4. Modelling of the frame

Figure 4 shows an overview of the OpenSees (Mazzoni *et al.* 2009) model with the details of the modelling strategy for the SC-CBs and the SC-BCJs (with PT bars). The modelling strategy for the FE modelling is based on a mixed lumped and distributed plasticity approach. Beams are modelled based on a lumped plasticity approach where the internal part of the beams is modelled as an *'elasticBeamColumn elements'*, while non-linear rotational springs '*zeroLength elements*' are placed at beams' ends. Columns are modelled with inelastic displacement-based *'nonlinearBeamColumn elements'* with four integration points. Each section is discretised into eight fibres along with the depth and four along each flange. Both beams and columns are defined by the *'Steel01'* material with 275 MPa and 355 MPa yield strength, respectively and 0.2% post-yield stiffness ratio. The *'section aggregator'* function accounts for the column's shear stiffness. The rigid-floor diaphragm is modelled by assigning a high value to the axial stiffness of the beams. Gravity loads are applied on the beams by considering the seismic combination of Eurocode 8. Lumped masses are concentrated at the floor nodes. Damping sources other than the hysteretic energy dissipation are modelled through the Rayleigh damping matrix, where the values of the mass-related and stiffness-related damping coefficients are considered for a damping factor of 3% for the first two vibration modes.

4.5. Modelling of the SC-BCJ

The SC-BCJ strategy modelling is shown in Figure 4 (b) and is consistent with Pieroni *et al.* 2022a. It consists of a simplified modelling strategy consisting of a non-linear rotational spring *'zeroLength'* element allocated at beams' ends and characterised by the flag-shape moment-rotation behaviour *'uniaxialMaterial SelfCentering'* considering: *1)* a rigid initial behaviour; *2)* the post-activation stiffness; *3)* the forward activation force corresponding to the moment at which the gap opening occurs, *i.e.,* M_1; 4) the ratio to reverse activation force; 5) no slippage and no bearing. The rigid elements of the joints are modelled with *'elastic beam-column elements'* with high flexural stiffness. Conversely, in the LD-MRF, the rotational springs are defined with a

'*uniaxial hysteretic material*' with symmetric trilinear force-displacement law. This material adopts a yielding force equal to the sliding force of the FDs and negligible post-elastic hardening to simulate the FDs' behaviour.

4.6. Modelling of the SC-CB

The SC-CB strategy modelling is shown in Figure 4 (a), and it is consistent with the validated strategy defined by Elettore *et al.* 2021a,b. The rocking interface is modelled with 8 rigid *'elastic beam-column elements'* with very high flexural stiffness. The web and flanges FDs are modelled with 4 translational springs represented by four *'zero-length elements'*. They are defined by the *'Steel01'* material considering a rigid initial behaviour, a low strain-hardening ratio, and a yield strength equal to the design slippage forces in the web and flanges FDs. The rocking behaviour is modelled with 4 translational springs *'zeroLength'* elements defined by the *'Compression-no-tension (ENT)'* material to capture the contact behaviour. The SC system is modelled with a single translational spring represented by a single *'zero-length'* element with bilinear elastic-plastic behaviour. It is defined by the *'Steel01'* material, with an elastic stiffness equal to the equivalent stiffness and the yield strength of the SC system. The initial PT force is modelled with the *'Initial strain material'*. It is highlighted that, in the case of LD-CBs, the joint is modelled without the central spring and adjusting the forces in the other springs to match the expected moment-rotation relationship.

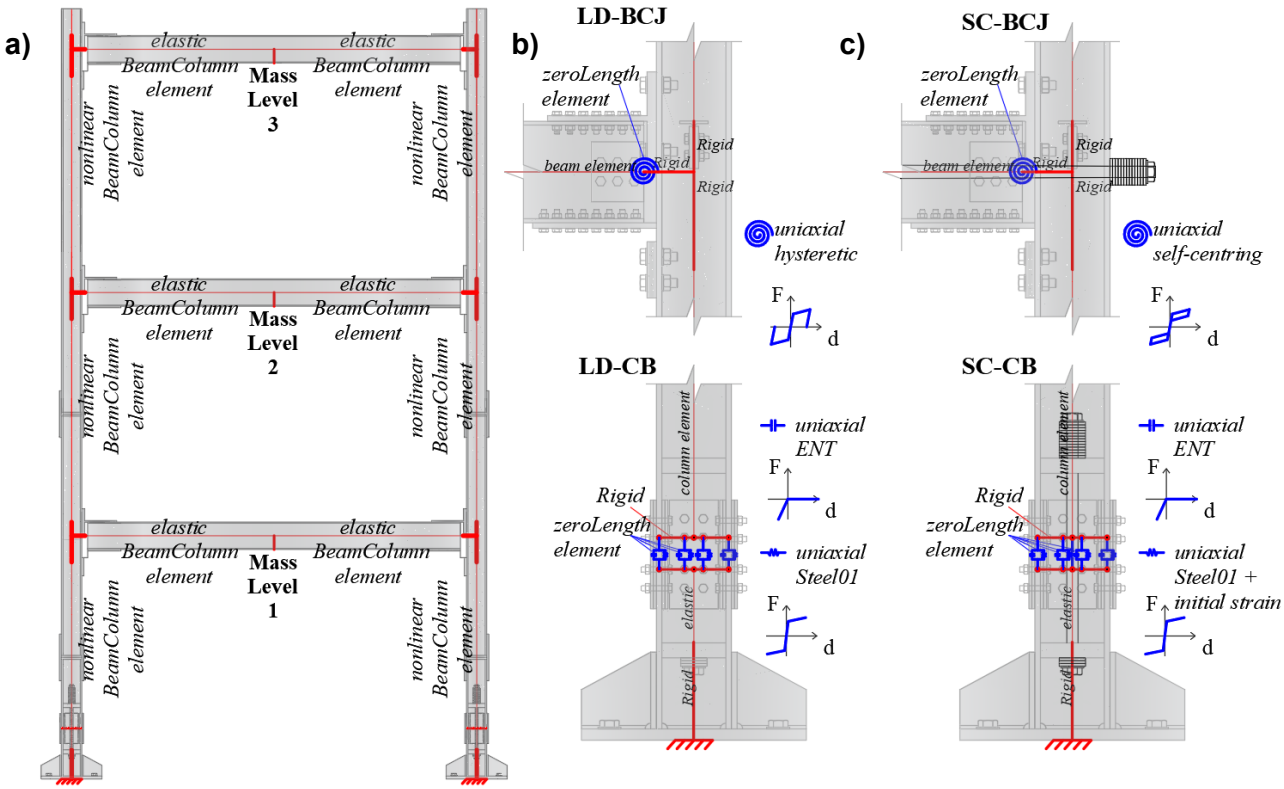

Figure 4. 2D OpenSees (Mazzoni et al. 2009) Modelling of: a) MRF; b) LD connections; c) SC connections.

5. Numerical Simulations

Non-linear dynamic analyses are performed for the three different configurations of the same structure: 1) the LD-MRF; 2) the LD-MRF-CB; 3) the SC-MRF. The three models have an almost identical natural vibration period T_1 = 0.43 sec. For this study, one single ground motion record is selected from a suite of 30 natural ground motion records selected from the SIMBAD Database (Iervolino *et al.* 2010). The mean elastic spectrum of the records set is kept between 75% and 130% of the corresponding Eurocode 8 elastic response spectrum. A large number of zero acceleration points are added at the end of each record to correctly capture the residual drifts. Figure 5 shows the Eurocode 8 elastic response spectrum and the spectra of the 30 accelerograms scaled at the ULS and CLS, respectively. In addition, the spectrum of the selected accelerogram is highlighted in black in both plots. Figure 6 shows the acceleration time history of the selected ground motion record scaled at the ULS and CLS. In all cases, the records are scaled in time by a scaling factor of $\lambda^{1/2} = 0.6^{1/2} = 0.77$.

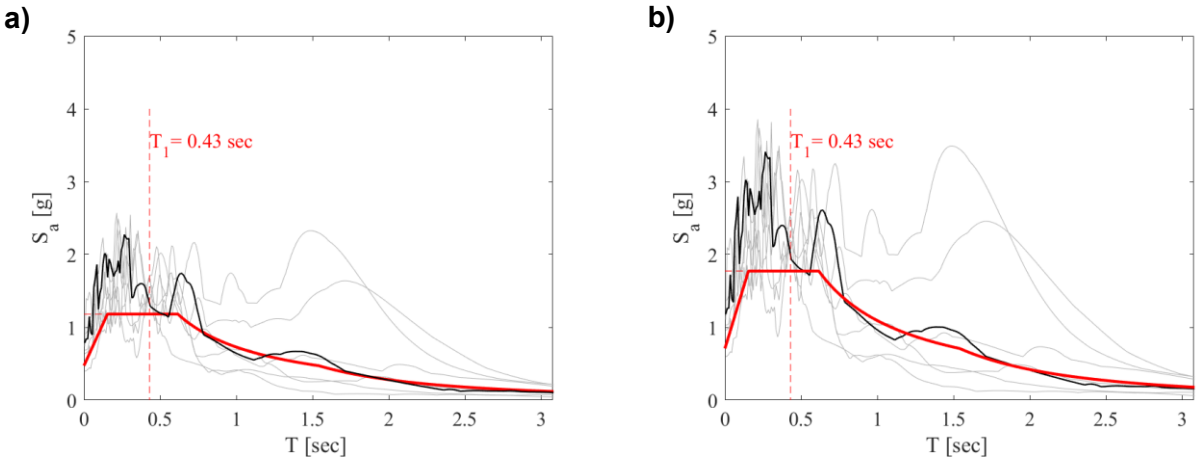

Figure 5. Spectra of the selected ground motion records scaled at the a) ULS and b) CLS.

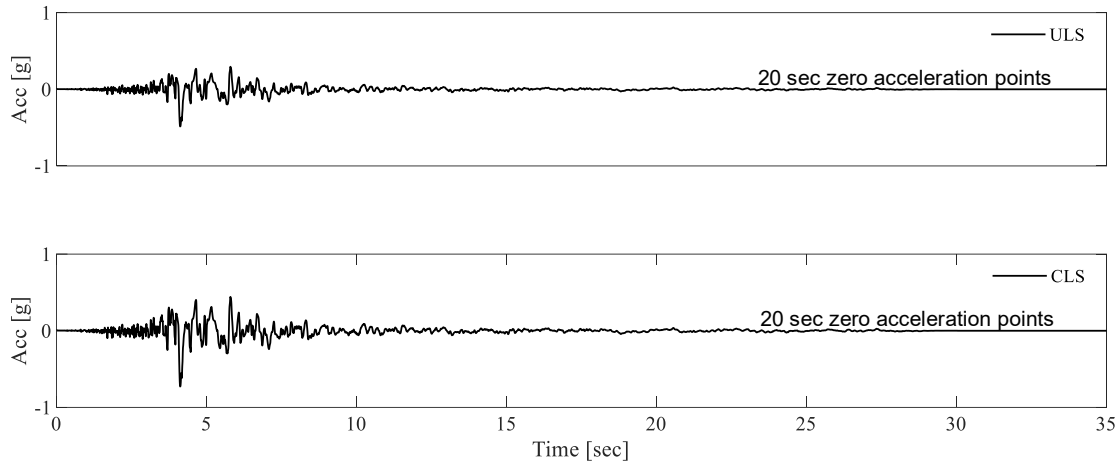

Figure 6. Acceleration history of the selected ground motion record scaled at the a) ULS and b) CLS.

For a single ground motion record, Figure 7 and Figure 8 compare the Interstorey Drifts (IDRs) time histories among the three configurations at the ULS and CLS intensities, respectively. Results demonstrate that in the LD-MRF-CB and SC-MRF, there is a significant reduction of the IDR at all the storeys and at both intensities of interest, confirming the results of previous research studies. The SC-MRF structure shows a completely self-centring response with residual IDRs equal to zero for both seismic intensities. Despite having SC joints only at the base (*i.e.,* only SC-CBs), the LD-MRF-CB shows a significant reduction of the residual drifts at all storeys. In particular, the LD-MRF-CB experiences residual interstorey drifts lower than the reparability limit of 0.5% for all the storeys, even at the CLS. Conversely, this limit is never satisfied at the CLS for the LD-MRF, which experiences residual IDRs higher than 0.5% even at the 1st storey. These preliminary numerical results provide useful information for the shake-table tests and on the expected behaviour of the specimen. It is expected that the curves related to the other configurations with different placements of SC-BCJs will result in between the responses of the LD-MRF-CB and the SC-MRF.

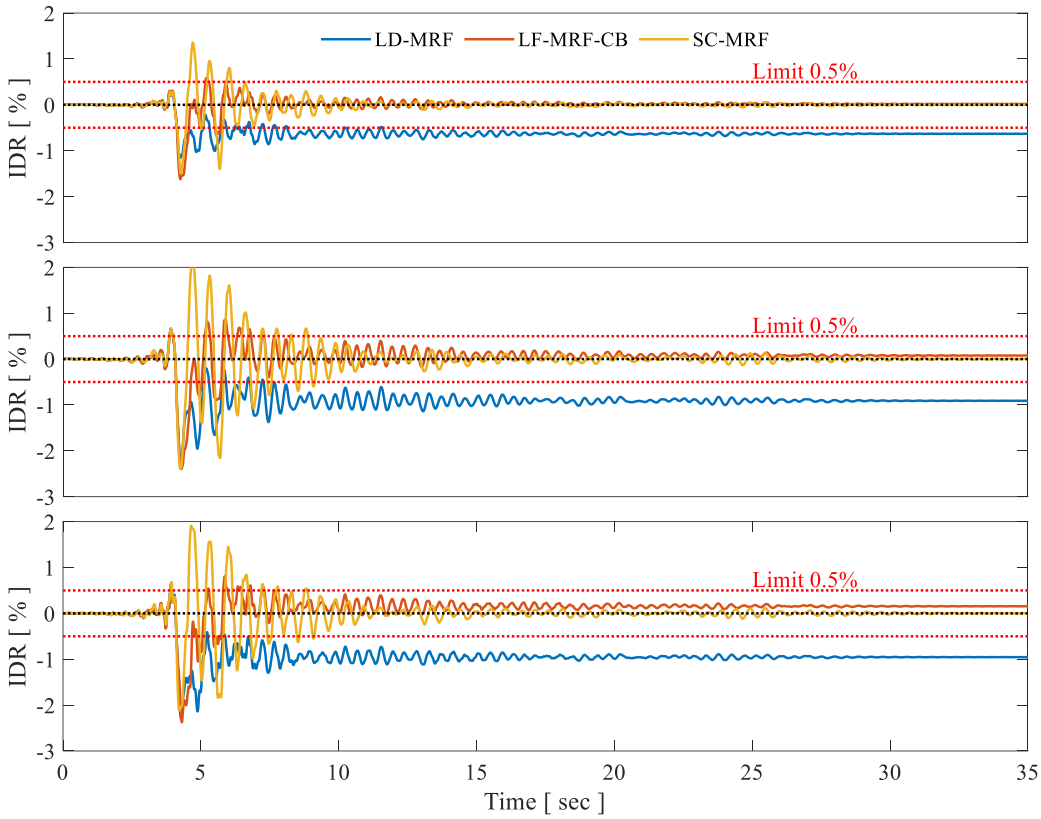

Figure 7. Comparison of the interstorey drifts (IDRs) time histories among the three configurations for a single ground motion record at the ULS

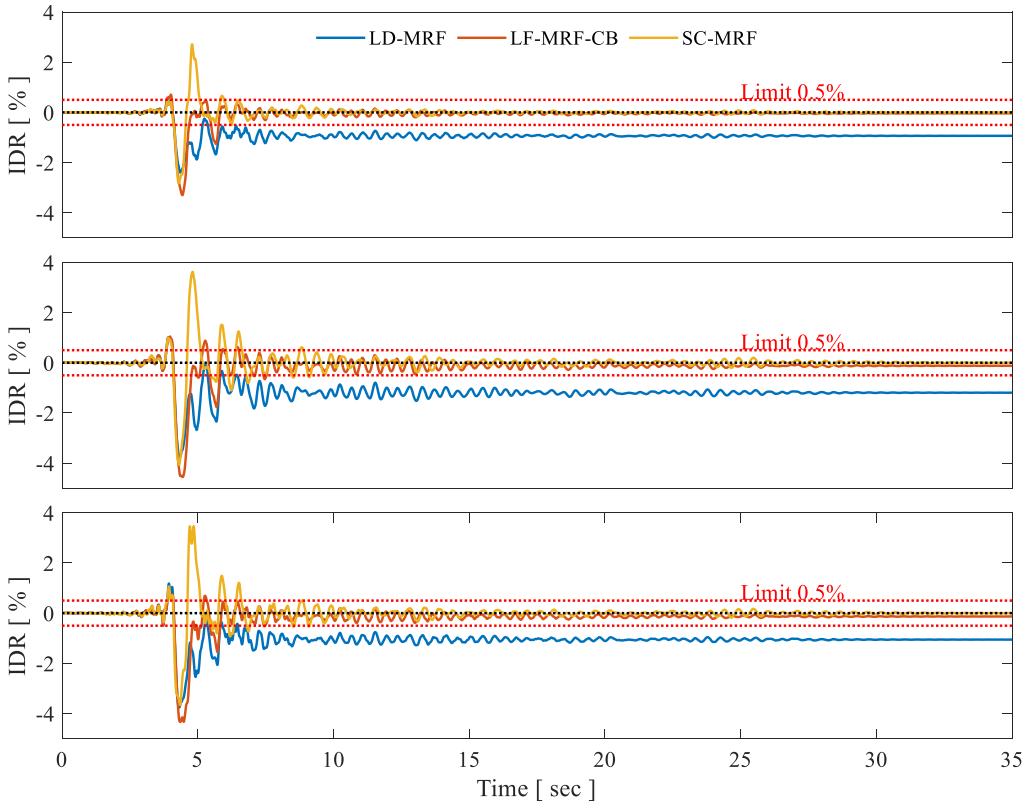

Figure 8. Comparison of the interstorey drifts (IDRs) time histories among the three configurations for a single ground motion record at the CLS

6. Conclusions

Within the context of the ERIES-SC-RESTEEL (Self-Centring seismic-RESilient sTEEL structures) project, a series of shaking table tests will be conducted on a large-scale three-storey steel MRFs with self-centring (SC) Beam Column Joints (BCJs) and Column Bases (CBs) considering different placements, configurations and properties of SC connections. The shaking table tests will be carried out at LNEC (Laboratório Nacional de Engenharia Civil) in Lisbon, Portugal, and aim to investigate the seismic performance of the structure but also evaluate the repairability (including the repair time) and the performance of the repaired structure through repeated tests. This paper illustrates the preliminary design of the test specimen, the test programme and some preliminary numerical analyses carried out on the structure. A Finite Element (FE) model of the test specimen is developed in OpenSees, and non-linear dynamic analyses are performed to investigate the performance of the structure considering three distributions of low-damage and low-damage self-centring joints within the specimen. The outcomes offer useful insights for the design of shaking table tests and for the prediction of the expected experimental results.

7. Acknowledgement

This work is part of the transnational access project “ERIES – SC-RESTEEL”, supported by the Engineering Research Infrastructures for European Synergies (ERIES) project (www.eries.eu), which has received funding from the European Union’s Horizon Europe Framework Programme under Grant Agreement No. 101058684. This is ERIES publication number C6.

8. References

Blomgren H.-E., Pei S., Jin Z., Powers J., Dolan J.D., van de Lindt J.W., Barbosa A.R., Huang D. (2019). Full-scale shake table testing of cross-laminated timber rocking shear walls with replaceable components. *Journal of Structural Engineering*, 145(10): 04019115.

CEN (2004). *EN 1998-1:2004. Eurocode 8: Design of structures for earthquake resistance - Part 1: General rules, seismic actions and rules for buildings*, Comité Européen de Normalisation, Brussels.

Christopoulos C., Filiatrault A., Uang C.-M., Folz B. (2002). Posttensioned energy dissipating connections for moment-resisting steel frames. *Journal of Structural Engineering*, 128(9): 1111–20.

Dall’Asta A., Leoni G., Gioiella L., Micozzi F., Ragni L., Morici M., Scozzese F., Zona A (2022). Push-and-release tests of a steel building with hybrid base isolation. Engineering Structures, 272: 114971.

Di Benedetto S., Francavilla A.B., Latour M., Piluso V., Rizzano G. (2022). Experimental response of a large-scale two-storey steel building equipped with low-yielding friction joints. *Soil Dynamics and Earthquake Engineering*, 152: 107022.

Elettore E., Freddi F., Latour M., Rizzano G. (2021a). Design and analysis of a seismic resilient steel MRFs equipped with damage-free self-centering CBs. *Journal of Constructional Steel Research*, 179: 106543.

Elettore E., Lettieri A., Freddi F., Latour M., Rizzano G. (2021b). Performance-based assessment of seismic-resilient steel MRFs equipped with innovative CB connections. *Structures*, 32: 1646-1664

Elettore E., Freddi F., Latour M., Rizzano G. (2022). Parametric Finite Element Analysis of Self-Centering Column Bases with different Structural Properties. *Journal of Constructional Steel Research*, 199: 107628

Elettore E., Freddi F., Latour M., Rizzano G. (2023). Pseudo-Dynamic Testing, Repairability, and Resilience Assessment of a Large-Scale Steel Structure Equipped with Self-Centering Column Bases. *Earthquake Engineering and Structural Dynamics*.

FEMA P58-1. (2012). *Seismic performance assessment of buildings. Volume 1 - Methodology*. Applied Technology Council, Redwood City, CA.

Freddi F., Dimopoulos C.A., Karavasilis T.L. (2017). Rocking damage‐free steel CB with friction devices: design procedure and numerical evaluation. *Earthquake Engineering and Structural Dynamics*, 46(14): 2281-2300.

Freddi F., Dimopoulos C.A,. Karavasilis T.L. (2020). Experimental Evaluation of a Rocking Damage-Free Steel CB with Friction Devices. *Journal of Structural Engineering*, 146(10): 1-20.

Garlock M., Sause R., Ricles J.M. (2007). Behavior and design of posttensioned steel frame systems. *Journal of Structural Engineering*, 133 (3): 389–399.

Gioiella L., Tubaldi E., Gara F., Dezi L., Dall'Asta A. (2018). Modal properties and seismic behaviour of buildings equipped with external dissipative pinned rocking braced frames. *Engineering Structures*, 172: 807–819.

Grant D., Fenves G., Whittaker A. (2004). Bidirectional modelling of high-damping rubber bearings. *Journal of Earthquake Engineering*, 8(1): 161-185.

Grigorian C.E., Yang T.S., Popov E.P. (1993). Slotted bolted connection energy dissipators. *Earthquake Spectra*, 9(3):491-504.

Gutiérrez-Urzúa L.F., Freddi F. (2022). Influence of the design objectives on the seismic performance of steel moment resisting frames retrofitted with buckling restrained braces. *Earthquake Engineering & Structural Dynamics*, 51(13): 3131–3153.

Iervolino I., Galasso C., Cosenza E. (2010). REXEL: Computer aided record selection for code-based seismic structural analysis, *Bulletin of Earthquake Engineering*, 8: 339–362.

Kamperidis V.C., Karavasilis T.L., Vasdravellis G. (2018). Self-centering steel CB with metallic energy dissipation devices. *Journal of Constructional Steel Research*, 149: 14-30.

Kim H.-J., Christopoulos C. (2009). Seismic design procedure and seismic response of post-tensioned self-centering steel frames. *Earthquake Engineering and Structural Dynamics*, 38: 355–376.

Kurama Y.C., Weldon Brad D., Shen Q. (2006). Experimental evaluation of posttensioned hybrid coupled wall subassemblages. *Journal of Structural Engineering*, 132(7), 1017-1029.

Latour M., D'Aniello M., Zimbru M., Rizzano G., Piluso V., Landolfo R. (2018). Removable friction dampers for low-damage steel beam-to-column joints. *Soil Dynamics and Earthquake Engineering*, 115: 66-81.

Latour M., Rizzano G., Santiago A., Da Silva L. (2019). Experimental response of a low-yielding, self-centering, rocking CB joint with friction dampers, *Soil Dynamics and Earthquake Engineering*, 116: 580–592.

Lettieri A., de La Peña A., Freddi F., Latour M. (2023). Damage-free self-centring link for eccentrically braced frames: development and numerical study. *Journal of Constructional Steel Research*, 201: 107727.

Li D., Zhou Y., Liu X., Simpson B.G., Xiao J. (2023). Experimental testing of GCr15 bearing steel with different surface treatments as passive friction energy-dissipative shims. *Construction and Building Materials*, 408: 133628.

MacRae G.A., Urmson C.R., Walpole W.R., Moss P., Hyde K., Clifton G.C. (2009). Axial Shortening of Steel Columns in Buildings Subjected to Earthquakes, *Bulletin of The New Zealand Society for Earthquake Engineering*, 42(4): 275–287.

MacRae G.A., Clifton G.C., Mackinven H., Mago N., Butterworth J.W., Pampanin S. (2010). The Sliding Hinge Joint Moment connection. *Bulletin of The New Zealand Society for Earthquake Engineering*, 43(3): 202–212.

Mazzoni S., McKenna F., Scott M.H., Fenves G.L. (2009). OpenSEES: Open System for earthquake engineering simulation. Pacific Earthquake Engineering Research Centre (PEER), University of California, Berkley, California. Available at http://opensees.berkeley.edu.

McCormick J., Aburano H., Ikenaga M., Nakashima M. (2008). Permissible residual deformation levels for building structures considering both safety and human elements. *Proceedings of the 14th World Conference of Earthquake Engineering*, Beijing, China.

O'Reilly G.J., Goggins J. (2021). Experimental testing of a self-centring concentrically braced steel frame. *Engineering Structures*, 238: 111521.

Ricles J., Sause R., Garlock M., Zhao C. (2001). Post-tensioned Seismic-Resistant Connections for Steel Frames. *Journal of Structural Engineering*, 127(2): 113–121.

Pampanin S., Ciurlanti J., Bianchi S., Perrone D., Granello G., Palmieri M., Grant D., Palermo A., Costa A., Candeias P., Correia A. (2023). Triaxial shake table testing of an integrated low-damage building system. *Earthquake Engineering and Structural Dynamics*, 52(10): 2983-3007.

Pieroni L., Freddi F., Latour M. (2022a). Effective placement of Self-Centering Damage-Free Connections for Seismic-Resilient Steel MRFs. *Earthuake Engineering and Structural Dynamics*, 51: 1292–1316.

Pieroni L., Di Benedetto S., Freddi F., Latour M. (2022b). Genetic algorithm for the optimal placement of Self-Centering Damage-Free joints in steel MRFs. *Journal of Constructional Steel Research*, 197: 107489.

Piras S., Palermo A., Saiidi M.S. (2022). State-of-the-Art of Posttensioned Rocking Bridge Substructure Systems. Journal of Bridge Engineering, 27(3): 03122001

Pei S., van de Lindt J. W., Barbosa A. R., Berman J. W., McDonnell E., Dolan J. D., Blomgren H.E., Zimmerman R. B., Huang D., Wichman S. (2019). Experimental Seismic Response of a Resilient 2-Story Mass-Timber Building with Post-Tensioned Rocking Walls. *ASCE Journal of Structural Engineering*, 145(11): 04019120.

Seo C.Y., Karavasilis T.L., Ricles J.M., Sause R. (2014) Seismic performance and probabilistic collapse resistance assessment of steel moment resisting frames with fluid viscous dampers. *Earthquake Engng Struct Dyn*, 43(14):2135-2154.

Shen Y., Freddi F., Li Y. (2022) Parametric experimental investigation of unbonded post-tensioned reinforced concrete bridge piers under cyclic loading. *Earthquake Engineering Structural Dynamic.* 51: 3479–3504.

Simpson B.G., Rivera Torres D. (2023). Simplified Modal Pushover Analysis to Estimate First- And Higher-Mode Force Demands for Design of Strongback-Braced Frames. Journal of Structural Engineering (United States), 147(12): 04021196.

Symans M.D., Charney F.A., Whittaker A.S., Constantinou M.C., Kircher C.A., Johnson M.W., McNamara R.J. (2008). Energy dissipation systems for seismic applications: Current practice and recent developments." *Journal of Structural Engineering*, 134(1): 3–21.

Wang Y., Zeng B., Zhou Z., Huang L., Yao J. (2022). Shaking table test of a three-story frame with resilient variable friction braces. *Journal of Constructional Steel Research*, 192: 107252.

Zhang R., Yan Z., Liu J., Xie J.-Y., Chouery K.E., Xiang P., Ramhormozian S., Jia L.-J. (2023). Seismic performance of a low-damage rocking column base joint along weak axis. Journal of Building Engineering. 67: 106056.